Cancer Chemother Pharmacol (1999) 43: 295–301

ORIGINAL ARTICLE

**Noriaki Tatsuta · Naomi Suzuki · Takae Mochizuki
Keizo Koya · Masayuki Kawakami · Tadao Shishido
Naomi Motoji · Hiroyuki Kuroiwa · Akiyo Shigematsu
Lan Bo Chen**

Pharmacokinetic analysis and antitumor efficacy of MKT-077, a novel antitumor agent

Received: 4 February 1998 / Accepted: 29 June 1998

Abstract MKT-077 (1-ethyl-2-{[3-ethyl-5-(3-methylbenzothiazolin-2-yliden)]-4-oxothiazolidin-2-ylidenemethyl} pyridinium chloride), a novel rhodacyanine dye in phase I/II clinical trials, may provide a new approach to cancer therapy based on the accumulation in the mitochondria of the cells of certain carcinomas, for example, those of the colon, breast and pancreas. To support the development of MKT-077 for clinical application as an intravenous (i.v.) therapy, we investigated the metabolic fate of [^{14}C]MKT-077 in BDF1 mice as well as the distribution of MKT-077 in experimental LS174T tumor-bearing mice using a high-performance liquid chromatography (HPLC) method. The plasma levels of ^{14}C after i.v. administration of [^{14}C]MKT-077 declined in a triphasic manner. In the first distribution phase, the levels of ^{14}C decreased with a $T_{1/2}$ of ~5 min. In the second and terminal phase, the $T_{1/2}$ of ^{14}C was 2.8–4.6 h and 16.2 h, respectively. C_{max} (1 min after injection) increased from 0.3 to 1.5 μg/ml linearly, but less than proportionately between the doses. The $AUC_{(0-\infty)}$ at 0.3, 1 and 3 mg/kg were 0.030 ± 0.002, 0.60 ± 0.12 and 1.73 ± 0.25 μg · h/ml, respectively. Plasma clearance was ~1.8 l/h per kg (at doses of 1 and 3 mg/kg). The steady state volume of distribution (6.8 and 25.1 l/kg) indicated that MKT-077 distributed as a lipid-soluble molecule. The mean residence time (MRT) was 4.1 (at a dose of 1 mg/kg) and 14.1 h (at a dose of 3 mg/kg). In the first rapid phase (5 min after dosing), ^{14}C radioactivity was detected in most of the tissues and organs, most strongly in the kidney cortex, and not in the central nervous system and testes. In the terminal phase (24 h after dosing), ^{14}C contents increased in the intestinal tract, and in the kidney and liver were nearly to the background level. After i.v. bolus administration at a dose of 3 mg/kg of [^{14}C]MKT-077, the predominant route of elimination of the radioactivity was via the feces, and recoveries of total radioactivity in urine and feces corresponded to 33.5% and 61.1%, respectively. More than 60% was recovered within 24 h and 95% within 1 week. MKT-077 was primarily excreted in unmetabolized form with five unidentified metabolites found in the urine and plasma. Intact MKT-077 was retained in the tumor tissue longer than in plasma and kidney in LS174T tumor-bearing mice receiving MKT-077 at an i.v. therapeutic dose (10 mg/kg). This accumulation decreased very slowly, suggesting that the high membrane potentials of tumor cell mitochondria may help retain the drug in tumors.

Key words MKT-077 · Mitochondria · Pharmacokinetics · Delocalized lipophilic cation · Antitumor agent

N. Tatsuta (✉). K. Koya
Shionogi BioResearch Corp.,
45 Hartwell Ave., Lexington,
MA 02173, USA
Tel.: +1-781-274-8200 (ext. 2272); Fax: +1-781-274-8228;
E-mail: tatsuta@erols.com

N. Suzuki · T. Mochizuki · K. Koya · M. Kawakami · T. Shishido
Ashigara Research Laboratories,
Fuji Photo Film Co., Ltd.,
210 Nakanuma, Minamiashigara,
Kanagawa, 250-01, Japan

N. Motoji · H. Kuroiwa · A. Shigematsu
Institute of Whole Body Metabolism,
340-2 Nauchi, Shiroi, Inba,
Chiba, 270-14, Japan

L.B. Chen
Dana-Farber Cancer Institute,
Harvard Medical School, 1 Jimmy Fund Way,
Smith Building, Room 1058,
Boston, MA 02115, USA

Introduction

The rhodacyanine dye 1-ethyl-2-{[3-ethyl-5-(3-methylbenzothiazolin-2-yliden)]-4-oxothiazolidin-2-ylidenemethyl} pyridinium chloride (MKT-077, Fig. 1) was developed as a novel antineoplastic compound against adenocarcinoma [1, 2]. In vitro, MKT-077 inhibits the growth of five human cancer cell lines based on a new mechanism of action: delocalized lipophilic cationic compounds (DLCs)

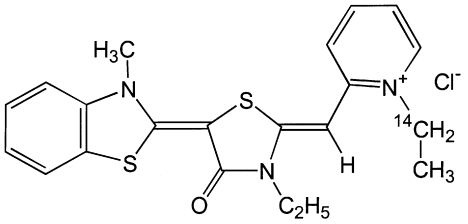

Fig. 1 Chemical structures of MKT-077 and [^{14}C]MKT-077

accumulate in the mitochondria in response to high negative mitochondrial membrane electrical potentials [3–5]. In nude mice, MKT-077 inhibits the growth of subcutaneously (s.c.) implanted A498 human renal carcinoma cells and DU145 human prostate carcinoma cells and prolongs the survival of mice bearing intraperitoneally (i.p.) implanted LOX human melanoma cells [6–9]. Phase I/II clinical trials are in progress.

To support the development of MKT-077 for clinical application as an intravenous (i.v.) therapy, we investigated the metabolic fate of [^{14}C]MKT-077 in BDF1 mice as well as the distribution of MKT-077 in experimental tumor-bearing mice. We examined the pharmacokinetics (disposition, distribution and excretion) of [^{14}C]-MKT-077 in male BDF1 mice, and the distribution in plasma, kidney and tumor of MKT-077 in tumor-bearing nude mice receiving MKT-077 i.v. at a therapeutic dose (10 mg/kg) using a high-performance liquid chromatographic (HPLC) assay system.

Materials and methods

Chemicals

Non-labeled MKT-077 was synthesized by Fuji Photo Film Kanagawa, Japan, and radiolabeled [^{14}C]MKT-077 was synthesized by Amersham (Fig. 1). The specific activity of [^{14}C]MKT-077 was 43.3 μCi/mg and the radiochemical purity, based on thin-layer chromatography (TLC), was more than 98.4%. The purity of MKT-077 was more than 99% based on HPLC.

Animals

Male BDF1 mice (7 weeks old) and female Balb/c nu/nu mice (5 weeks old) were obtained from SLC Japan, Edogawa, Tokyo. Animals were acclimated for approximately 1 week prior to use. BDF1 mice were fed laboratory chow (CE-2; CLEA Japan, Meguro, Tokyo), and water ad libitum, and were housed in temperature- and humidity-controlled rooms (22 ± 10 °C, 60 ± 10%). Balb/c nu/nu mice were fed laboratory chow (CFR-1; Oriental Yeast, Itabashi, Tokyo, Japan), and water ad libitum, and were housed in temperature- and humidity-controlled rooms (22 ± 20 °C, 55 ± 15%).

Disposition study

[^{14}C]MKT-077 was diluted with non-labeled MKT-077 and prepared as a solution in saline for injection (JSP grade). Five mice were used for each dose. [^{14}C]MKT-077 solution was injected i.v. via a tail vein. The dose was adjusted based on each animal's body weight (0.3 mg/kg dose, 13.0 μCi in 5 ml; 1.0 mg/kg dose, 43.4 μCi in 5 ml; 3.0 mg/kg dose, 129.3 μCi in 5 ml). Blood samples (20–300 μl) were collected at intervals of 1, 5, 10 and 30 min and 1, 2, 4, 6, 8, 24, 48 and 72 h after administration of the compound. After centrifugation (5000 rpm, 8 min) of whole blood samples to obtain plasma, radioactivity was measured in all plasma samples using a liquid scintillation counter (model Aloka LSC-1000) after dissolving 10–100 μl plasma in 10 ml dioxane-type scintillator cocktail with external standard quench correction. The radioactivity levels were converted to the equivalent concentrations of MKT-077 (ng eq/ml).

The plasma samples (5 min after 3 mg/kg dosing) were extracted using methanol after lyophilization. The extract and [^{14}C] MKT-077 were separated by TLC on silica gel 60 F_{254} (Merck, TLC Art. 5715, Merck, Darmstadt) using chloroform/methanol (4/1, v/v). The TLC plate was placed in contact with an imaging plate (Fuji Photo Film Co.) and analyzed using a Bio-imaging analyzer BAS-2000 (Fuji Photo Film Co.) to measure the distribution of radioactivity.

Pharmacokinetic analysis

The results are expressed as the mean values and standard deviation (SD). The half-life ($T_{1/2}$) was estimated at $0.693/k$, where k is the least square regression of the log-linear concentration time points. The area under curve (AUC) was calculated using the modified trapezoidal method [10]. The portion of AUC from the last measurable plasma concentration to infinity was estimated as C/k, where C represents the last measurable plasma concentration. Plasma clearance (CL_p) was calculated as the dose divided by total $AUC_{(0-\infty)}$. The apparent volume of distribution at steady-state (Vd_{ss}) and the mean residence time (MRT) were determined according to a previously described method [11, 12].

Excretion study

After i.v. administration of [^{14}C]-MKT-077 (3 mg/kg), the mice ($n = 3$) were housed in metabolic cages. Urine and feces were collected at 24, 48, 72, 96 and 168 h (1 week) after administration. CO_2 in expired air was collected in a series of two traps containing monoethanolamine solution. The traps were replaced at the same time as the collection of urine and feces.

The radioactivity in the urine was counted directly and in feces was counted after homogenization with water. The radioactivity from $^{14}CO_2$ was counted in the monoethanolamine solution. The radioactivity of each sample was determined using a liquid scintillation counter (model Aloka LSC-1000) after dissolving the sample in 10 ml liquid scintillation cocktail.

The urine samples (24 h after i.v. dosing) were analyzed by TLC on silica gel 60 F_{254} (Merck, Art. TLC 5715) using chloroform/methanol (4/1, v/v). The TLC plate was placed in contact with an imaging plate (Fuji Photo Film Co.) and analyzed using a Bio-imaging analyzer BAS-2000 (Fuji Photo Film Co.) to measure the distribution of radioactivity.

Distribution study

A [^{14}C]MKT-077 solution was injected into three male BDF1 mice i.v. via a tail vein at a dose of 3 mg/kg (131.4 μCi/mg, 5 ml/kg). The mice were euthanized under ether anesthesia at 5 min, 6 h and 24 h after i.v. dosing. The mice were then frozen in liquid nitrogen and kept in a freezer (−20 °C). The limbs and tails were removed and the carcass was embedded in 5% carboxymethyl cellulose solution on the stage of a microtome and frozen in liquid nitrogen. The sections were placed in contact with an imaging plate (Fuji Photo Film Co.) and analyzed using a Bio-imaging analyzer BAS-2000 (Fuji Photo Film Co.).

Distribution in LS174T-bearing nude mice

Human colon carcinoma LS174T was obtained from Dr. Shuji Kojima (Research Institute for Bioscience, Science University of Tokyo). Human xenografts were propagated by s.c. serial transplantation in female Balb/c nu/nu mice. On day 0, tumors were carefully trimmed to remove all connective tissues, cut into frag-

ments of 3 mm^3 and implanted s.c. using a 12-gauge trocar needle. On day 11, these mice were used in the distribution study.

MKT-077 was injected intravenously via a tail vein into three mice at a dose of 10 mg/kg (2 ml/kg). Animals were euthanized at 2, 24 and 48 h after administration of drug. Upon sacrifice, blood samples (300 µl) were collected and the kidneys and tumors were removed. After centrifugation of whole blood (5000 rpm, 8 min), the plasma was separated and stored at −20 °C until analysis. The kidneys and tumors were weighed, and stored at −20 °C until analysis.

Determination of MKT-077 in plasma samples

Each plasma sample (100 µl) was transferred to a 1.5-ml centrifuge tube. Acetonitrile (200 µl) containing glacial acetic acid (0.6% solution, v/v) was added and the sample mixture was vortexed well and centrifuged for 5 min at 3000 rpm. After centrifugation, the supernatant was filtered and transferred into another centrifuge tube. The filtrate (150 µl) was diluted with water (150 µl) containing acetonitrile, glacial acetic acid and triethylamine (20 m*M* solution) and mixed well. Then 50 µl of the solution was loaded onto the HPLC system comprising a reverse-phase column (TSK-gel, ODS-80TM, 4.6 mm × 50 mm; Tosoh, Chuo, Tokyo, Japan) with a guard column (Guard-Pak C18; Waters). The mobile phases consisted of methanol/water (60/40, v/v) containing 0.2% triethylamine and acetic acid (pump LC-9A; Shimadzu Seisakusho). The flow rate was 1 ml/min. MKT-077 was detected at the visible wavelength of 490 nm (detector SPD-10AV; Shimadzu Seisakusho). The Retention time of MKT-077 was 8.5 min. The column temperature was controlled at 40 °C. The peak was integrated using a data processor (C-R4A Chromatopak; Shimadzu Seisakusho, Kyoto, Japan). The results are expressed as the mean values and SD.

Determination of MKT-077 in kidney and tumor samples

Stored tissue samples were thawed at room temperature. Each sample was homogenized with a threefold weight of 50% DMSO solution (v/v) at 700 rpm for 2 min. Then a fourfold weight of acetonitrile containing glacial acetic acid (0.6% solution, v/v) was added to the mixture, and the mixture was vortexed well and agitated. After centrifuging the mixture at 1000 rpm for 10 min at 4 °C, the supernatant was applied to a SEP-PAK C_8 (Waters, Shinagawa, Tokyo, Japan) column preconditioned with 5 ml methanol containing glacial acetic acid (0.6% solution, v/v) followed by 10 ml acetic acid and triethylamine solution (20 m*M*). Then the column was washed with 10 ml acetic acid and triethylamine solution (20 m*M*) and dried by passing air through. The column was washed with 1 ml methanol containing glacial acetic acid (0.6% solution, v/v). Finally, 50 µl water was added to the eluate, and 50 µl of the solution was loaded onto the HPLC system described above.

Antitumor activity against LS174T human colon carcinoma xenografts

MKT-077 was administered i.v. to LS174T-bearing nude mice ($n = 6$/group) every other day between days 1 and 20 at doses of 5, 7.5 and 11.25 mg/kg. Antitumor activity was assessed on the basis of mean tumor weight changes between day 1 and the final day of evaluation relative to the control. The results are expressed as the mean values and SD. Student's *t*-test was used to evaluate the differences between the means from the control and treatment groups.

Results

Plasma pharmacokinetics of [^{14}C]MKT-077

Figure 2 shows the plasma levels of radioactivity after i.v. administration of [^{14}C]MKT-077 at doses of 0.3, 1 and 3 mg/kg to male BDF1 mice. The pharmacokinetic parameters obtained from compartmental analysis are shown in Table 1. Because the plasma profiles were not fully defined at the doses of 0.3 and 1 mg/kg, the terminal elimination constants defined by those data were used to calculate the residual AUC, clearance and MRT for each dose. The radioactivity level of the plasma declined in a triphasic manner at the dose of 3 mg/kg. The $T_{1/2}$ values of ^{14}C materials in the rapid (α, 1–10 min), slower (β, 1–8 h), and terminal (γ, 8–72 h) phases were 4.1–4.8 min (0.3–3 mg/kg), 2.8–4.6 h (1 and 3 mg/kg) and 16.2 h (3 mg/kg), respectively. C_{max} increased from 0.3 to 1.5 µg/ml linearly, but less than proportionately between the doses. $AUC_{(0-\infty)}$ at doses of 0.3, 1 and 3 mg/kg were 0.030 ± 0.002, 0.60 ± 0.12 and 1.67 ± 0.25 µg · h/ml, respectively. The CL_p value was 1.4–1.6 l/h per kg (at doses of 1 and 3 mg/kg). The Vd_{ss} values (6.8 and 25.1 l/kg) indicated that MKT-077 distributed as a lipid-soluble molecule. The MRT was 4.1 h at a dose of 1 mg/kg and 14.1 h at 3 mg/kg.

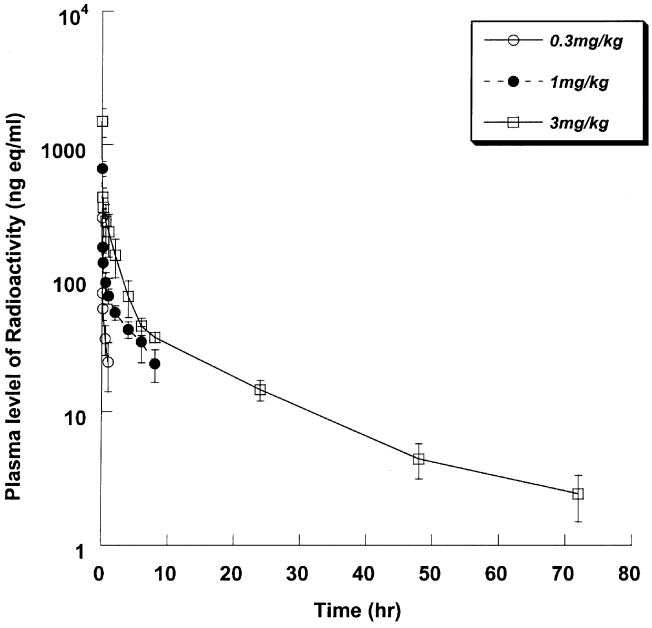

Fig. 2 Plasma levels of radioactivity after i.v. administration of [^{14}C]MKT-077

The contents of metabolites in the plasma samples (5 min after injection) are shown in Table 2. The recovery of the extraction method was 83.7%. More than 50% of extracted material consisted of MKT-077. Five spots which appeared to be metabolites were detected by TLC, and the major metabolite was M-1. The radioactivity detected at the origin by TLC included impurity of the administered material.

Distribution of [^{14}C]MKT-077

Figure 3 shows whole-body autoradiograms at 5 min, and 6 and 24 h after i.v. bolus injection of [^{14}C]MKT-

Table 1 Pharmacokinetic data for MKT-077 after administration of single doses in male mice (values are means ± SD from five animals)

Route	Dose (mg/kg)	C_{max}^{a} (ng/ml)	$T_{1/2\alpha}$ 1–10 min (min)	$T_{1/2\beta}$ 1–8 h (h)	$T_{1/2\gamma}$ 8–72 h (h)	$AUC_{(0-\infty)}$ (μg · h/ml)	CL_p (l/h/kg)	Vd_{ss} (l/kg)	MRT (h)
Bolus i.v.	0.3	281.0 ± 42.9	4.4 ± 1.0	– [b]	– [b]	0.030 ± 0.002	10.0 ± 0.8	2.7 ± 0.7	0.3 ± 0.1
	1.0	689.4 ± 86.4	4.1 ± 0.3	4.6 ± 1.4	– [b]	0.60 ± 0.12	1.7 ± 0.4	6.8 ± 0.8	4.1 ± 1.1
	3.0	1494.4 ± 369.3	4.8 ± 1.6	2.8 ± 0.7	16.2 ± 2.3	1.73 ± 0.25	1.8 ± 0.3	25.1 ± 6.5	14.1 ± 2.1

[a] The blood samples were taken 1 min after i.v. administration
[b] Radioactivity was not detected in these phases

Table 2 Composition of metabolites in plasma and urine after i.v. administration of MKT-077 at a dose of 3 mg/kg

Metabolite	Rf value	Plasma content (%) at 5 mm	Urine content (%) at 24 h
M-1	0.57	10.7	19.0
MKT-077	0.26	55.8	51.8
M-2	0.10	3.2	11.7
M-3	0.09	3.7	6.1
M-4	0.04	3.4	2.9
Origin	0.00	15.7	5.3
Concentration of radio-activity in Plasma (ng eq/ml)		380	
Recovery (%)		83.7	100

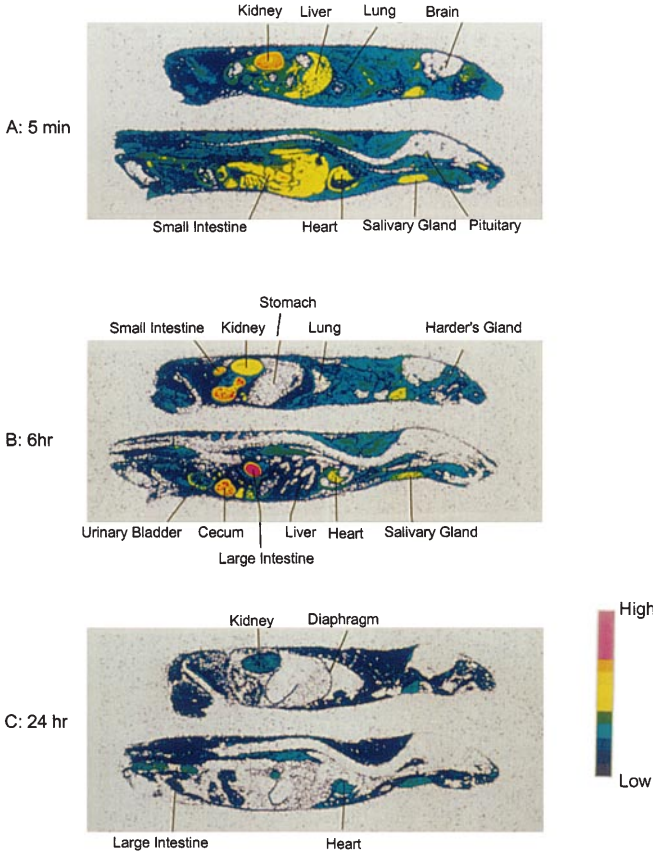

Fig. 3A–C Whole-body autoradiograms after i.v. administration of [^{14}C]MKT-077 to mice at a dose of 3 mg/kg. **A** 5 min, **B** 6 h, **C** 24 h (*upper* left lateral aspect, *lower* central axial aspect)

077 to three male BDF1 mice. Radioactivity was detected in most tissues and organs 5 min after injection. Tissues and organs that had high radioactivity were the kidney, liver, thyroid, brown fat, heart, salivary gland, pituitary, tongue, urine in the urinary bladder, pancreas, stomach, the contents of the cecum, intestinal wall and the contents of the intestine. Radioactivity in the central nervous system (CNS) and testes was at background levels at all observation time-points. Although the renal cortex and the liver had high concentrations of radioactivity at 5 min, ^{14}C levels had declined by 6 h, especially in the liver. The liver and lung did not retain high levels of ^{14}C-labeled material 24 h after injection. At 24 h after injection, kidney, salivary gland, skeletal muscle tissue, diaphragm and heart retained low levels of ^{14}C-labeled material.

Excretion of MKT-077

The cumulative excretion of radioactivity in the urine and feces after i.v. bolus injection of [^{14}C]MKT-077 at a dose of 3 mg/kg to male BDF1 mice is shown in Table 3. About 61.1% of the radioactivity was excreted in the feces. About 33.5% of the dose was recovered in the urine. The excretion of radioactivity in expired air as $^{14}CO_2$ was 0.3% of the dose within 168 h of administration. Total radioactivity in the urine, feces and expired CO_2 recovered within 168 h of administration was about 95% of the dose.

The contents of metabolites in the urine samples 24 h after administration at a dose of 3 mg/kg are shown in Table 2. More than 50% of the extracts consisted of MKT-077. Five spots, which appeared to be metabolites, were detected by TLC, and the major metabolites

Table 3 Cumulative excretion of radioactivity after i.v. administration of [^{14}C] MKT-077 at a dose of 3 mg/kg. Values are percent of administered dose ± SD (*NC* not counted)

Time (h)	Urine	Feces	Respired air	Total
6	16.1 ± 2.0	NC	NC	16.1 ± 2.0
24	26.2 ± 1.4	42.1 ± 2.2	0.1 ± 0.0	68.4 ± 1.3
48	30.0 ± 0.9	53.8 ± 1.7	0.2 ± 0.1	84.1 ± 2.0
72	31.6 ± 0.6	56.4 ± 1.2	0.3 ± 0.1	88.2 ± 1.5
96	32.0 ± 0.6	58.1 ± 1.2	0.3 ± 0.1	90.4 ± 1.5
168	33.5 ± 0.7	61.1 ± 0.9	0.3 ± 0.1	95.0 ± 1.0

Table 4 Tissue distribution of MKT-077 in LS174T-bearing nude mice after i.v. administration at a dose of 10 mg/kg

	Time after injection (h)		
	2	24	72
Plasma (ng/ml)	148.0 ± 3.2	53.2 ± 3.5	9.0 ± 4.1
Kidney (μg/g)	124.7 ± 16.3	69.0 ± 10.4	6.0 ± 1.3
Tumor (μg/g)	2.8 ± 1.1	1.3 ± 0.7	0.7 ± 0.6

were M-1 and M-2. The radioactivity detected at the origin on the TLC plate included impurity of the administered material.

Distribution of MKT-077 in LS174T-bearing nude mice

The tissue distribution of MKT-077 in the plasma, kidney and tumor after i.v. administration are summarized in Table 4. The validity of the HPLC method was indicated by the linearity of the standard curves (20–1000 ng/ml for kidney samples, $r = 0.995$; 20–1000 ng/ml for tumor samples, $r = 1.000$; and 2.5–600 ng/ml for plasma samples, $r = 0.9998$). The recovery of MKT-077 in these samples ranged from 75 to 100%.

Concentrations of MKT-077 in the kidney and tumor were higher than that in plasma, indicating that MKT-077 behaves as a lipophilic molecule, which supports the results of the whole-body autoradiography described above. At 2 h after i.v. administration, the concentration of MKT-077 in the tumor was 2.8 ± 1.1 μg/g tissue, in the kidney was 124.7 ± 16.3 μg/g tissue and in the plasma was 148.0 ± 3.2 ng/ml. The ratio of MKT-077 in the tumor to that in the plasma was approximately 19, which increased to 23 at 24 h after administration.

Antitumor activity against LS174T human colon carcinoma xenografts

The response of human colon carcinoma LS174T s.c. xenografts to i.v. treatment with MKT-077 is shown in Fig. 4. MKT-077 showed increasing antitumor activity against LS174T at doses of 5, 7.5 and 11.25 mg/kg. At 11.25 mg/kg tumor growth was markedly inhibited ($P < 0.05$).

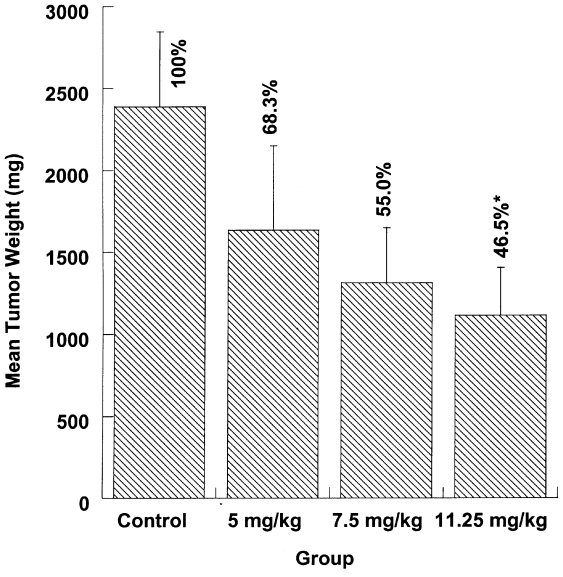

Fig. 4 Antitumor activity of MKT-077 against LS174T human colon tumors (*$P < 0.05$)

Discussion

We examined the pharmacokinetics (disposition, excretion and metabolism) of MKT-077 in male mice and its distribution in tumor-bearing mice as a preclinical model species.

Although the plasma concentration profiles were not fully defined at the low doses, the plasma levels of [^{14}C]MKT-077 declined in a triphasic manner at a dose of 3 mg/kg. In the first distribution phase, the levels of ^{14}C decreased with a $T_{1/2}$ of ~5 min. In the second and terminal phase, the $T_{1/2}$ of ^{14}C was 2.8–4.6 h (at 1 and 3 mg/kg) and 16.2 h (at 3 mg/kg). The C_{max} and AUC were less than proportional between the doses. The correlation between these parameters suggested that at least two factors, protein binding and excretion rate, especially metabolic rate, contributed to the differences in C_{max} and AUC linearity. The Vd_{ss} (6.8 and 25.1 l/kg) indicated that [^{14}C]MKT-077 (including metabolites) distributed as a lipid-soluble molecule. In the first rapid phase (5 min after dosing), ^{14}C radioactivity was detected in most of the tissues and organs, most strongly in the kidney cortex, but not in the CNS and testes. The observation of behavior changes in preclinical toxicity studies might be due to this rapid distribution to the organs but not the CNS [13, 14].

In the terminal phase (24 h after dosing), ^{14}C contents increased in the intestinal tract, but in the kidney and liver were nearly at the background levels. Higher levels of [^{14}C]MKT-077, which was found to be MKT-077 from the nude mice study data, in the kidney indicate some specificity for renal cells, that may be related to the renal toxicity. Some parameter changes relating to renal toxicity have been observed but neither neurotoxicity nor myelotoxicity have been seen in preclinical toxicology studies in rodents or dogs (unpublished results).

In order to enter the brain, drugs must pass through the endothelial cells of the capillaries of the CNS, the so-called blood-brain barrier (BBB); there are no slit junctions, unlike in the liver and spleen. Therefore, the chemical nature of the drug strongly influences its ability to cross the membrane. Although the Vd_{ss} of [^{14}C]MKT-077 and autoradiograms after i.v. injection indicate that this drug should behave as a lipophilic molecule able to cross the BBB, [^{14}C]MKT-077 did not distribute in the CNS, and probably did not pass through the barrier.

This phenomenon could be explained by the following. The partition coefficients of MKT-077 (log P = −1.6) [6] indicate the ability to penetrate the BBB and permeate fatty tissue such as CNS drugs are able to do [15]. However, the water-soluble (>200 mg/ml in water) [2, 6] property and the positive charge may prevent MKT-077 from passing through the BBB. Also, P-glycoprotein (Pgp) may mediate the efflux of MKT-077, as well as other DLCs such as Rh123, from the endothelial cells of the capillaries of the CNS [16]. Pgp has been found in hepatocytes and renal cells in in vitro studies using Rh123 [17, 18]. It would be of interest to investigate whether Pgp plays a role in the transport of MKT-077 into the brain, in biliary and renal excretion and in the distribution of MKT-077. Such studies could be conducted using *mdr*1 knockout mice and Pgp modulators such as cyclosporin A and verapamil [19, 20].

After i.v. bolus administration of [^{14}C]MKT-077 at a dose of 3 mg/kg, the predominant route of elimination of radioactivity was via the feces with 61.1% of the dose eliminated in 1 week, probably via bile, based on the data from rats (unpublished data). Urinary excretion was the secondary excretion pathway with 33.5% of the dose eliminated within 1 week. Elimination via CO_2 exhalation was 0.3% of the dose within 168 h after administration, indicating that oxidative de-ethylation seldom occurs in this ethylpyridinium moiety. MKT-077 was primarily excreted as the unmetabolized form with five unidentified metabolites found in the urine and plasma. No attempt has successfully identified the chemical structure of these metabolites. More than 60% was recovered within 24 h and 95% within 1 week. Slow excretion of MKT-077 from the tissues may be due to retention in the mitochondria, which appear to be a reservoir for DLCs [5]. A prediction from these observations is that MKT-077 may show pharmacological activity when injected every other day as well as every day [6]. In comparison with excretion in rats and dogs, the elimination rate and the amount of metabolites of [^{14}C]MKT-077 in mice were similar to those in dogs but faster than those in rats (unpublished data).

We also examined the distribution of MKT-077 in the plasma, kidney and tumor in tumor-bearing nude mice receiving MKT-077 at an i.v. therapeutic dose (10 mg/kg). MKT-077 showed a significant but not large efficacy against this tumor in our animal study (Fig. 4). The tumor concentration of MKT-077 was much lower than that in the kidney. It may be significant to show antitumor activity against and distribution studies in tumors such as human renal carcinoma, since Koya et al. [6] have demonstrated significant activity of MKT-077 against this tumor in nude mice. The ratio of MKT-077 in the tumor to that in the plasma was about 19, which was lower than that of Rh123 using different s.c. tumor-bearing mice [20]. It will be of interest to examine if the drug has efficacy against naturally occurring tumors such as those of the colon, stomach and liver [21] because MKT-077 distributed in these tissues well. It is noteworthy that, while the accumulation in the tumor was small, the accumulation decreased very slowly, suggesting that the high membrane potentials of tumor cell mitochondria may not only play a role in retaining the drug in the tumor but also serve as a slow-release device for MKT-077 [5].

Acknowledgements We thank Mr. Daijiro Nishio, Mr. Toshinao Ukai and Mr. Akihiko Ikegawa for their suggestions and Dr. Shuji Kojima for the supply of LS174T. We also want to acknowledge Ms. Hitomi Ikenaga and Dr. Yoichi Matsumoto for their technical assistance.

References

1. Kawakami M, Koya K, Ukai T, Tatsuta N, Ikegawa A, Ogawa K, Shishido T, Chen LB (1997) Synthesis and evaluation of novel rhodacyanine dyes that exhibit antitumor activity. J Med Chem 40: 3151
2. Kawakami M, Koya K, Ukai T, Tatsuta N, Ikegawa A, Ogawa K, Shishido T, Chen LB (1998) Structure-activity of rhodacyanine dyes as antitumor agents. J Med Chem 41: 130
3. Chen LB (1988) Mitochondrial membrane potential in living cells. Annu Rev Cell Biol 21: 155
4. Wong JR, Chen LB (1988) Recent advances in the study of mitochondria in living cells. Adv Cell Biol 2: 263
5. Chen LB (1989) Mitochondria as a reservoir for anticancer drugs. Anticancer Drugs 191: 21
6. K. Koya K, Li Y, Wong H, Ukai T, Tatsuta N, Kawakami M, Shishido T, Chen LB (1996) MKT-077, a novel rhodacyanine dye in clinical trials, exhibits anticarcinoma activity in preclinical studies based on selective mitochondrial accumulation. Cancer Res 56: 538
7. Modica-Napolitano JS, Koya K, Weisberg E, Brunelli BT, Li Y, Chen LB (1996) Selective damage to carcinoma mitochondria by rhodacyanine MKT-077. Cancer Res 56: 544
8. Weisberg EL, Koya K, Modica-Napolitano J, Li Y, Chen LB (1996) In vivo administration of MKT-077 causes partial yet reversible impairment of mitochondrial function. Cancer Res 56: 551
9. Modica-Napolitano JS, Brunelli BT, Koya K, Chen LB (1998) Photoactivation enhances the mitochondrial toxicity of cationic rhodacyanine MKT-077. Cancer Res 58: 71
10. Yeh KC, Small RD (1989) Pharmacokinetic evaluation of stable piecewise cubic polynomials as numerical integration functions. J Pharmacokinet Biopharmacol 17: 721
11. Perrir D, Mayersohn M (1982) Noncompartmental determination of the steady-state volume of distribution for any mode of administration. J Pharm Sci 71: 372
12. Gibaldi M, Perrier D (1982) Noncompartmental analysis based on statistical moment theory. In Swarbrick J (ed) Pharmacokinetics, 2nd edn. Marcel Dekker, New York, p 409
13. Gamboa-Vujicic G, Emma DA, Liao SY, Fuchtner C, Manetta A (1993) Toxicity of the mitochondrial poison dequalinium chloride in a murine model system. J Pharm Sci 82: 231
14. Castro DJ, Saxon RE, Rodgerson DO, Fu YS, Bhuta SM, Fetterman HR, Castro DJ, Tartell PB (1989) Rhodamine-123 as a new laser dye: in vivo study of dye effects on murine metabolism, histology and ultrastructure. Laryngoscope 99: 1057
15. Hansch C, Leo A (1979) Partition coefficients; substituent constants for correlation analysis in chemistry and biology. John wiley & Sons, New York, p 169
16. Fontaine M, Elmquist WF, Miller DW (1996) Use of rhodamine 123 to examine the functional activity of P-glycoprotein

in primary cultured brain microvessel endothelial cell monolayers. Life Sci 59: 1521
17. Ernest S, Bello-Reuss E (1995) Expression and function of P-glycoprotein in a mouse kidney cell line. Am J Physiol 269: C323
18. Yamazaki M, Suzuki H, Sugiyama Y (1996) Recent advances in carrier-mediated hepatic uptake and biliary excretion of xenobiotics. Pharm Res 13: 497
19. Jette L, Beaulieu E, Leclerc JM, Beliveau R (1996) Cyclosporin A treatment induces overexpression of P-glycoprotein in the kidney and other tissues. Am J Physiol 270: F756
20. Vora MM, Dhalla M (1992) In vivo studied of nonlabeled and radiolabeled rhodamine-123. Int J Radial Appl Instrum [B] 19: 405
21. Chiba Y, Kubota T (1996) Antitumor activity of MKT-077, a delocalized lipophilic cation, against human tumor cells. In: Proceeding of the Japanese Cancer Association 55th Annual Meeting October, 1996 Yokohama, The Japanese Cancer Association, Tokyo, Japan, p. 189